Introduction to zeolite theory and modelling

Chapter 9

INTRODUCTION TO ZEOLITE THEORY AND MODELLING

R.A. VAN SANTEN

Laboratory of Inorganic Chemistry and Catalysis,
Eindhoven University of Technology,
P.O. Box 513, 5600 MB Eindhoven, The Netherlands

D.P. DE BRUYN, C.J.J. DEN OUDEN, B. SMIT

Koninklijke/Shell-Laboratorium, Amsterdam (Shell Research B.V.),
P.O.Box 3003, 1003 AA Amsterdam, The Netherlands

I. INTRODUCTION

Solid-state inorganic chemistry is undergoing a renaissance. This is partly due to important innovations in material science, such as the discovery of high-temperature superconductors, new developments in ceramics and, last but not least, the advent of new zeolites for catalysis and separation. Another significant factor is the availability of large computer power and appropriate theoretical chemistry programs that allow the computation of electronic and atomic properties with sufficiently high accuracy to be of chemical interest. Combined with graphics facilities this enables the visualization of complex chemical structures, which is very useful to the crystallographer as well as the chemist who whishes to manipulate the zeolitic materials.

In this chapter we will present an introduction to the methods currently available to study zeolites theoretically. Whereas some of the methods to be discussed have been used for more than 25 years, the applications to zeolites, with their large unit cells, are only of quite recent date. For this reason, the possibilities as well as the limitations of the use of computational chemistry in zeolite science are still being assessed.

Questions relating to the degree of ionicity and covalency of the metal-oxide bond are again the subject of major dispute. We will see how different approaches emphasize one or the other aspect and where possible we will indicate potential ways for further development.

The comparison of spectroscopic measurements on zeolites with theoretical results computed for the same system is a powerful way to progress. The many structures possible for zeolites with non-varying composition such as the silicon zeolites, make them a favoured testing material of interest to inorganic chemistry as a whole.

In the first section we will start with a discussion of theoretical methods to compute the stability of zeolite lattices. Insight into zeolite lattice

stability is important to understand the dependence of zeolite topology on composition. It clearly is of relevance if one wishes to predict the stability of unknown structures. It is important to realize that because of the microporous nature of the zeolite structure, the channels and cavities will be readily filled with molecules if in contact with a liquid or gas. For instance, if a zeolite is synthesized, it will be in contact with its mother liquor. The chemical potential of the zeolite will depend on zeolite lattice stability as well as on its interaction with the molecules enclosed.

In the next sections methods to compute or estimate the interaction of the zeolite lattice and cations occluded in the zeolite channels with adsorbed molecules will be discussed.

Initially we will focus on the interaction potentials to be used; later statistical mechanics using Monte Carlo simulations will be discussed. In the section on zeolite stability, theoretical studies on the position of the channel cations neutralizing zeolite lattice charge will also be discussed. Such studies were the first to demonstrate clearly the effectiveness of solid-state chemical techniques to predict zeolite structural features.

Zeolites are of catalytic interest because they can act as solid acids. Acidity appears to be a function of zeolite composition and possibly also of zeolite structure. Several methods to predict acidity will be dealt with and their relative merits assessed. Particularly the relevance of long-range electrostatic interactions versus short-range local changes in chemical bonding environment will be discussed.

We have not included a discussion on fractals in our chapter, because zeolite micropores are crystallographically well defined and consequently regular. The concept of fractals has been defined for irregular structures. It may be of interest to study induced fractal behaviour if one blocks channels or microcavities by preadsorption, but we consider this to be outside the scope of our discussion. An analysis of fractal behaviour in zeolites can be found in ref. 1.

Computer simulation of adsorbed molecules and diffusion requires the use of molecular mechanics and molecular dynamics techniques as well as computer modelling facilities. The latter possibilities will be presented and they will be illustrated in the consecutive sections on adsorption and diffusion.

The chapter will be concluded with a brief discussion of future perspectives in zeolite theory as well as applications to zeolite catalysis.

Emphasis in this chapter will be on the introduction of a particular theoretical method in the context of a theoretical problem to be studied, rather than on an in-depth treatment of the theoretical background of such a method. For those interested we have included appropriate references.

II. THEORY ON ZEOLITE LATTICE STABILITY

Zeolite structures can be regarded as networks formed by the interconnection of silica rings consisting of four, five or six rings. Whereas hypothetical zeolite structures containing three rings have been proposed and minerals having three-ring silicate units exist, so far for zeolites they have not been found in nature, nor have they been synthesized. Using three rings, zeolite structures can be built with large channel dimensions (ref. 2), so it is in principle of interest to know whether such structures can be stable. There is a considerable body of work devoted to the question of the relative stability of silica ring systems and we will address this problem in this section.

Secondly, whereas silicalite can be crystallized with a very low Al content, this is not the case for faujasite. This structure is found in zeolites X and Y, and can only directly be made with a high aluminium content. So the question of the relative stability of silicate rings as a function of aluminium concentration is of interest. Because of charge neutrality for each Al^{3+} in substituting for Si^{4+} in the zeolite lattice, additional positive charge has to be introduced in the form of positively charged intra-channel cations. As we will see, the relative stability of these cations depends on the local environment of the cations concerned.

There are two approaches to the computational study of complex inorganic structures. One starts with the ionogenic nature of the attractive part of the chemical bonds. In addition, Born-type repulsive interactions are introduced so that equilibrium distances can be calculated. Covalent interactions are considered corrections and are accounted for by the additional introduction of Van der Waals interaction terms or by explicit incorporations of polarization. The other approach has as its starting point the quantum-chemical nature of the chemical bond. Approximate quantum-chemical approaches followed are usually limited to clusters. Only recently have practical schemes applicable to infinite lattices been implemented.

The rigid-ion and shell-model approaches to be discussed first (ref. 3) are based on the first philosophy. Bonding is assumed to be mainly ionic, so the potential used consists of a long-range electrostatic term and a short-range covalent one. The long-range term due to Coulomb interactions is calculated using an Ewald summation of the electrostatic potentials due to point charges (ref. 3c). The short-range potential that is employed is of a Buckingham type:

$$\Phi^{s}_{ij} = A_{ij}\exp(-r_{ij}/\rho_{ij}) - C^{(6)}_{ij}/r^{6}_{ij} \qquad \text{(II.1)}$$

where r_{ij} is the distance between atoms i and j, and A_{ij}, $C^{(6)}_{ij}$ and ρ_{ij} are short-range parameters. The repulsive term in (II.1) is of a Born-repulsion-interaction type characterized by an exponential r_{ij} dependence. The

attractive term describes the Van der Waals interaction between two polarizable atoms.

To study zeolites, it is essential, according to some authors (ref. 3b), to introduce in addition the "bond-bending" term:

$$\Phi(\theta) = k\ (\theta - \theta_o)^2 \qquad \text{(II.2)}$$

where $E(\theta)$ is the bond-bending energy, θ is the O-Si-O bond angle and θ_o is the tetrahedral angle. The term imparts a degree of "tetrahedrality" to the SiO_4 groups.

The approximations for the potentials used so far constitute the rigid-ion model. One can also include ionic polarizabilities, as is done in the shell model. According to this model the ion is thought to consist of a core and a massless shell interconnected by a "spring". The shell has a charge Y and the core has a charge equal to Z-Y, where Z is the total ionic charge. Usually, the spring is considered to be harmonic. The polarization of a free ion is related to the charges and spring constant by:

$$d = (Ye)^2 / 4\pi\epsilon_o K \qquad \text{(II.3)}$$

where d is the ionic polarizability, Y the shell charge, e the unit charge, ϵ_o the vacuum permittivity, and K the core-shell harmonic spring constant. In the shell model, the Buckingham potential and the bond-bending three-body potential are defined between shells and not between cores.

With these potentials the technique of lattice energy minimization (ref. 3a) is used to compute interatomic distances and angles and to predict some physical properties, such as the dielectric constant and the elasticity constants. The forces on the atoms are computed and an iterative procedure is used to converge atom positions to those locations where the energy is minimized and the forces on the atoms disappear.

The main difference between rigid-ion and shell-model calculations is that the shell model decreases the effective charges to be used in the Ewald summation ($\approx$ 80%) and computes a frequency-dependent dielectric constant, which also causes the Coulomb interactions to decrease (ref. 4).

The parameters to be used in eqs. (II.1) and (II.2) are fitted to give good unit cell dimensions as well as elastic constants. Full formal charges are used to compute the electrostatic interactions.

A method related to the shell-model energy-minimization method is the method of contraints investigated by No and Jhon and co-workers (ref. 5). The parameters of the potential energy function are defined by the constraint method and are obtained by minimizing the function:

$$\Sigma_{i=1}^{k} \Sigma_{l=1}^{N} \Sigma_{j=1}^{3} d/d\alpha_i\ (\Phi^o/dq_j^{ol}) = F \qquad \text{(II.4)}$$

α_i is the i^{th} potential parameter and q_j^l and q_j^{ol} are the j^{th} coordinate of the l^{th} atom and that of the equilibrium structure, respectively. Φ^o is the potential energy function. In this method, the atom positions are assumed to be fixed and they are usually taken from experimental data. Potential parameters are then derived from eq. (II.4) by minimization of the total energy. Now in general the forces on the atoms will not disappear after minimization.

In the No-Jhon method, the Coulomb interaction is computed using charges derived from quantum-mechanical or other methods, e.g. using Hurley's electronegativity set (ref. 6a) or Sanderson's electronegativity equalization method (ref. 6b,c). The polarization energy is not computed using the shell model but from expression:

$$\Phi_{pol} = -1/2 \; \Sigma_{l=1}^{N} \alpha_l \; [\; (\Sigma_{j=1}^{N} E_{lj}^{x})^2 + (\Sigma_{j=1}^{N} E_{lj}^{y})^2 + (\Sigma_{j=1}^{N} E_{lj}^{z})^2 \;] \qquad (II.5)$$

α_l is the polarizability of atom l and E_{lj}^{u} the component of the electric field along the u direction (u=x,y,z) at position l due to an atom on position j. Instead of a Buckingham potential, the short-range potential is calculated from a Lennard-Jones (6-12) type potential:

$$\Phi = \Sigma_l \; \Sigma_{j>l} \; \epsilon_{lj} \; [\; (\sigma_{lj}/r_{lj})^{12} - (\sigma_{lj}/r_{lj})^{6} \;] \qquad (II.6)$$

The rigid-ion as well as the constraint method has been applied to the calculation of cation positions in zeolite Y (ref. 3c), zeolite X (refs. 3c,7) as well as mordenite (ref. 8).

The K^+ position in zeolite X lattices was investigated using Madelung energy calculations as well as rigid ion minimization of the cation position in an otherwise fixed structure. Comparison of different positions shows that the S_{II} site at the centre of the six-rings that project outward into the supercage is energetically favoured by most of them. The S_I and $S_{I'}$ sites, one with the hexagonal prism, the other linked to a hexagon but within the sodalite cage, appear to be equally occupied.

Other investigations of aluminium-rich zeolites concern Sr^{2+} and Na^+ (ref. 3c). Usually very good agreement with experiment is found and a clear discrimination between potential sites can be given.

Replacement of Na^+ by Ba^+ results in a destabilization (ref. 3c), as expected on the basis of a comparison of ionic radii.

The one detailed calculation that is available for low-Al-content mordenite (ref. 8) indicates that it is more important for the Ni^{2+} ion to have an environment that compensates its charge by the close approximation of two Al ions in its coordination shell than to occupy a specific extra framework position.

It should be noted that in zeolites with a high framework Al concentration the interaction between the extra framework cations themselves may significantly affect the relative stability of different cation positions. This has also been noted in a study where the Madulung energy of ZSM, mordenite and faujasite lattices was computed as a function of cation content (Na^+) (ref. 9). The compensating lattice charge was calculated by varying the average lattice cation charge, dependent on Na^+ concentration. On sodium and oxygen full formal charges were used. One finds that the electrostatic energy of the faujasite lattice is relatively insensitive to cation content, but that of mordenite or ZSM-5 strongly decreases with high Al/Si ratio. This is due to a smaller micropore volume of the channels in ZSM-5 and mordenite, which cannot accommodate as many cations as the faujasite micropores. As a result, large repulsive effects between cations appear in the high-density structures if the cation concentration is high.

Once parameters are available one can try to use similar modelling techniques to those developed for the modelling of organic molecules to predict zeolite framework or cation conformations. Free-valence geometry molecular mechanics calculations have been recently carried out on a sodalite cage cluster (ref. 10). In this method the potentials between framework atoms are essentially harmonic and an electrostatic potential, containing a dielectric constant is added. Mabilia, Pearlstein and Hopfinger (ref. 11) used charges and force constants derived from organo-silicon compounds. The structures were determined using energy minimization techniques. A study was made with varying Al/Si ratio. It appears that the conformational stability of the sodalite cage increases with aluminium content, which does not seem to agree with experiment. This indicates a need for a more extensive study of the potentials to be used, a subject which we will revert to later on.

Rigid-ion and shell-model calculations have also been used to compute the lattice stability of zeolites (ref. 12). Energy minimization of a few silica zeolites, polymorphs of quartz, shows that the stability of the most open structure (faujasite) and the most dense structure (α-quartz) differs by $\approx$ 40 kJ/mol SiO_2 according to rigid-ion theory and only by $\approx$ 20 kJ/mol SiO_2 according to the shell-model theory. Note that these results have been obtained with full formal charges on the ions.

Comparison of computed and experimental lattice infrared spectra shows reasonable agreement between shell-model and experimental spectra (refs. 4,13). The agreement is especially good for the bending modes. The vibrational models deviate on average by 10 %. An experimental probe for the long-range electrostatic field is the computed vibrational plasmon frequency. The shell-model value is lower than the rigid-ion value, but still deviates by a factor of 6 from the experimental values. Although this is probably not critical for

computed lattice stabilities, it is important for theories of acidity and catalysis in zeolites as well as lattice dynamics.

Jhon and No and co-workers applied the constraint method to derive potentials for $AlPO_4$-5 (ref. 14). They applied their potentials to compute vibrational spectra for clusters derived from zeolite-A (ref. 15). However, no computations are available to test experimental and computed spectra on zeolite lattice vibrations. Therefore the accuracy of their potentials is difficult to judge.

There is an extensive body of literature on alternative potentials to be used. Here we will mention the work of Lee (ref. 16), who determined a two- as well as three-body potential for crystalline silica, and the work of Garofalini (ref. 17) on glass. Both derive empirically determined potentials. According to Lee one expands the potential as a function of two-, three-, or n-body potentials:

$$\Phi = 1/2!\ \Sigma_i^N \Sigma_j^N u(r_i,r_j) + 1/3!\ \Sigma_i^N \Sigma_j^N \Sigma_k^N u(r_i,r_j,r_k) + \ldots + 1/n!\ \Sigma_i^N \Sigma_j^N \ldots \Sigma_n^N u(r_i,r_j,\ldots,r_n) \qquad (II.6)$$

In all procedures discussed earlier the total potential was considered to be the sum of two body potentials $u(r_i,r_j)$ and an angular-dependent term approximating the three-body potential $u(r_i,r_j,r_k)$. These approximations imply that part of the existing dependence on three-body and higher potential terms has been incorporated in the potential constants that are empirically fitted. So a priori there is no guarantee that potentials based on such a procedure are transferable. One may even question whether it is useful to derive the transferable potentials or should limit oneself to different potentials dependent on the local environment studied. The last philosophy has been used by Clementi to determine H_2O-macromolecule interaction potentials based on ab-initio quantum chemical calculations (ref. 18).

Lee approximated $u(r_{ij})$ by a Mie-type potential:

$$\Phi(r_{ij}) = \epsilon/(m-n)\ [\ n(r_o/r_{ij})^m - m(r_o/r_{ij})^n\ ] \qquad (II.7)$$

and the three body-term as:

$$\Phi_1(r_i,r_j,r_h) = Z_1\ (1+3\cos\theta_i\cos\theta_j\cos\theta_h)\ /\ (r_{ij}r_{ih}r_{jh})^3 \qquad (II.8)$$

This form of Φ_1 represents the dominant triple dipole interaction (ref. 19).

A number of crystalline silica properties were computed using these potentials, with parameters derived partly from Si, O_2 and O_3 and from fitting the experimental cohesive energies of low-cristobalite and low-quartz.

Using the Monte-Carlo techniques to be discussed later temperature-dependent calculations as well as surface-stability calculations were performed.

Garofalini (ref. 17) used two body potentials for molecular dynamics calculations, a method to be discussed later, on v-SiO_2 and glass surfaces (ref. 20). Use was made of a modified Born-Mayer-Huggins potential function of the form:

$$\Phi_{ij} = (1+Z_i/n_i+Z_j/n_j)b_{ij}\exp((\sigma_i+\sigma_j-r_{ij})/\tau) + Z_iZ_je^2\exp(r_{ij}/(0.175L)) \qquad (II.9)$$

where Z is the electronic charge, n is the number of valence shell electrons, σ is the atom size, and L is the box size (molecular dynamics parameter), u is an empirical constant and b_{ij} the short-range repulsive parameter. Values of these parameters can be found in the literature (ref. 21). Usually a correction term is added appropriate for the Ewald summation. Some properties such as cohesive energy are reasonably well reproduced, but internal pressures are calculated too high, which is found to depend sensitively on the b parameter. Whereas potential (II.9) has a form suitable for molecular dynamics calculations, it follows from our earlier discussion that the short-range interactions are not described very well.

A first-principle approach to derive potentials is to do quantum chemical electronic structure calculations and compute total energies as a function of relative coordinates.

Although techniques exist to perform electronic structure calculations on quartz (ref. 22) and small unit cell silica polymorphs, these techniques have not yet been applied to derive effective interatomic potentials.

Currently two studies are available that compute bulk properties of crystalline silica based on potentials derived from quantum-chemical cluster calculations. An early study is that of Newton, O'Keeffe and Gibbs (ref. 23). Accurate calculations on the Hartree-Fock level have been done on the $H_6Si_2O_7$ molecule. By computing the total energy as a function of Si-O bond length and Si-O-Si angle, force constants for deformation of the Si-O-Si angle can be derived. These may be expressed as an Si...Si interatomic force constant. The above authors apply an analytical procedure to compute the bulk modulus of α-quartz and cristobalite and find a fair agreement. This illustrates that macroscopic properties depend mainly on proper values of short-range potential parameters. In the calculation of, among others Newton (ref. 23) no long-range electrostatic interactions had to be included.

A more recent study concerns a first-principles interatomic potential for silica, which also contains long-range electrostatic contributions (ref. 24). The potential was derived from a calculation on SiO_4^{4-} surrounded by four point charges. The potential used is similar to expression (II.1) to which a Coulomb term is added.

The important differences from the rigid-ion calculations are firstly that now charges of -1.2 on O and 2.4 on Si are used instead of the full formal charges; secondly, the short-range parameters have been derived from fitting to

the potential of the SiO_4 cluster, with proper accounting of the electrostatic interaction terms which are also present. Although computed bulk properties are satisfactory, the computed lattice vibrational spectrum is inferior to that computed with the classical shell model (ref. 4).

Although promising, the quantum-chemical approach has to be extended before derived potentials can be considered acceptable.

In order to establish the presence of strain effects in the silica-tetrahedron rings from which silica zeolites can be considered to be constructed, Van Beest et al. (ref. 25) computed energy-minimized configurations of $[SiO(OH)_2]_n$ ring systems using the GAMESS ab-initio programs. It appears that if the rings are allowed to minimize their strain, there is less than one kJ/mol energy difference between tetrahedra in four, five and six-tetrahedra rings. A three-tetrahedra ring appears to be destabilized by 10 kJ/mol tetrahedron.

So quantum-chemical as well as shell-model calculations basically confirm each other. The energy difference between SiO_2 zeolites is very small. The absence of three-tetrahedra rings in silica zeolites appears to confirm their lower energy.

One can also study changes in energy of tetrahedra containing rings or strings, with relative coordinates derived from experimental zeolite diffraction data. This has been demonstrated by, among others, Zamaraev (ref. 26), who argued that these clusters have to be considered to be embedded in the zeolite lattice, making them rigid. So far it has not been investigated how many distances can relax in zeolites, if substitutions of framework atoms occur. The driving forces are considerable. This follows from fully relaxed three-tetrahedera ring calculations, with one Si atom replaced by Al, charge compensated by a proton or Na^+ (ref. 4). The calculations show a significant weakening of the T-O bond upon substituting Al for Si.

A large deformation of the ring occurs not only if Si is replaced by Al, but also if Na^+ is replaced by a proton. The calculations also indicate that there exist large three-body potential terms, implying that effective two-body potentials strongly depend on the local environment.

Assuming non-relaxability of clusters and strings Derouane (ref. 27) and O'Malley (ref. 28), among others, compared total energy changes upon substitution of Al for Si at specific lattice positions, simulated by the string or ring cluster. Derouane finds preferential pairing of two Al atoms in a four-tetrahedra ring cluster; O'Malley also derives preferential positions. Similar computations were done by Beran (ref. 29), who used semi-empirical CNDO-2 calculations.

Whereas there appears to be significant progress in the development of potentials for SiO_2 zeolites, currently there is no potential available that

can reliably be used in computations not aiming to calculate lattice framework stability. This will become more apparent if we discuss the interaction of the zeolite framework with organic molecules and the acidity problem.

We mentioned earlier that methods based on a dominantly ionogenic picture of the SiO bond result in excellent predictions of alkali siting at extra framework positions in zeolites with a relatively high Al/Si ratio. Quantum-chemical calculations confirm the essential electrostatic interaction of Ni^{2+}, Mg^{2+} or K^{+}. The computed charges are close to the formal charges (refs. 30,4).

Although parameters for Al-O and P-O potentials exist no comparison with experiment (e.g. lattice vibration spectroscopy) is yet available that verifies their reliability. It is possible to derive potentials and charges also for non-purely SiO_2 systems from quantum-chemical cluster calculations. Such potentials may be expected to become available in the near future.

III. THEORY ON ADSORPTION AND ACIDITY

Bonding between the zeolite lattice and organic molecules adsorbed in the zeolite cavities is best described as Van der Waals-type weak interactions, in the case that interaction solely occurs with the silicon zeolite wall. The bonds should be considered to be hydrogen bonds if interaction occurs with the acidic protons in the zeolite. Interaction with the non-framework cations belongs to a category of bonding in between these two extremes.

Intermolecular interactions between medium-sized systems is a field of research that rapidly develops mainly in the context of interactions between molecules of biological interest. The quantum-chemical basis of these interactions with inorganic materials is relatively little explored. The most extensive work is due to Sauer (refs. 30, 31) and co-workers, which we will discuss below.

Hobza and Zahradnik (ref. 32) recently gave an extensive review on non-empirical calculations of weak interaction energies. On the basis of extensive studies they conclude that Hartree-Fock level ab-initio calculations provide reliable interaction energies, even with the use of limited basis sets, if proper corrections are made for the basis set superposition error ϵ(BSSE) and the Van der Waals interaction is explicitly included:

$$\delta E_w = \delta E(SCF) - \epsilon(BSSE) + E^D \qquad (III.1)$$

Computation of δE(SCF) using the Huzinaga minimal basis set (ref. 33) is recommended. Using this basis set, ϵ(BSSE) arising in quantum-chemical calculations if systems interact is minimized.

The basis set superposition error of the energy can be computed using Boys and Bernardi's function counterpoise method (ref. 34).

Since the Van der Waals E^D interaction is due to the correlated motion of electrons in the two interacting fragments, it is not included in the Hartree-Fock approximation. E^D is computed from the expression:

$$E^D = -\Sigma_i^R \Sigma_j^T C_{ij}^{(6)} R_{ij}^{-6} \qquad \text{(III.2)}$$

where R and T label the interacting fragments, and i and j the atoms from which they are constructed. R_{ij} are the interatomic distances. $C_{ij}^{(6)}$ is the coefficient including e.g. the polarizabilities and ionization potentials of atoms i and j.

The atomic polarizabilities can be readily determined from the bond or total polarizabilities. It has to be determined for particular valence states of the atoms (ref. 35). In ref. 35c computed values of $C_{ij}^{(6)}$ are tabulated for CH_4, C_3H_8 and NH_3 with excellent agreement with experiment. Table 1 lists atomic polarizabilities and ionization potentials for H, C, N, O and P as a function of valence state. $C_{ij}^{(6)}$ is computed from the London expression. If one does not use modified values for the atoms bonded in the molecule, E^D is underestimated by 50 %. The London expression for $C_{ij}^{(6)}$ is:

$$C_{ij}^{(6)} = -3h/2\ [I_iI_j/(I_i+I_j)]P_iP_j \qquad \text{(III.3)}$$

with I_i and P_i being the ionization potential and polarizability of atom i in the relevant valence state.

TABLE 1

Values of Atomic Polarizabilities (α) and Ionization Potentials (I) for the Following Atoms: H,C,N,O and P

atom	valence state[a]	α(Å^3)	I(eV)
H	σ	0.386	13.61
C	tetetete	1.064	14.57
	trtrtrπ[b]	1.382	11.22
	trtrtrπ[c]	1.230	11.22
	trtrtrπ[d]	1.529	11.22
	didi$\pi\pi$	1.279	11.24
N	te^{2}tetete	1.094	14.31
	trtrtrπ^2	1.090	12.25
	tr^{2}trtrπ	1.030	14.51
	di^{2}di$\pi\pi$	0.852	14.47
O	te^{2}te^{2}tete	0.664	18.40
	tr^{2}tr^{2}trπ	0.460	17.25
	tr^{2}trtrπ^2	0.422	14.97
	te^{2}te^{2}te^{2}te	1.791	6.31
P	teteteπ	1.743	12.09

[a] te = tetrahedral, tri = trigonal, di = diagonal. [b] Aliphatic hydrocarbons with double bond. [c] Aromatic hydrocarbon. [d] Condensed hydrocarbon.

It is of interest to note that the $\delta E(SCF)$ value may be approximated by its electrostatic interaction term as long as the interaction energy is calculated at distances larger than the Van der Waals minimum.

A detailed account of this electrostatic approximation has been given recently by Dykstra (ref. 37). Approximating $\delta E(SCF)$ by the electrostatic part of the interaction energy requires high quality calculations with large basis sets. A useful addition to the electrostatic approximation is expression (II.1), with $C_{ij}^{(6)}$ computed according to ref. 20.

An application of expression (III.1) can be found in ref. 31a. Here the interaction of H_2O with -SiOH and -Si-O-Si groups is discussed. Models used are disiloxane, $H_3Si-O-SiH_3$ and silicic acid. The interaction energies and H_2O complex geometries were determined and are summarized in Table 2.

TABLE 2

Energy Characteristics (in kJ/mol) for the Complex Formation

	Complex	ΔE (4-31G)	$\Delta\epsilon$	E^D	ΔE^{tot}
I	$H_2O...H_2O$	-33.47	-5.14	-6.86	-35.19
II	$(H_3Si)_2O...H_2O$	-22.51	-5.52	-14.18	-31.17
III	$Si(OH)_4...OH_2$	-38.20	-5.06	-6.70	-39.84
IV	$Si(OH)_4...H_2O$	-34.31	-10.62	-12.12	-35.81

Whereas expression (III.1) is very useful to determine local interactions between cluster models of a zeolite and interacting molecules, one requires analytical expressions for the interaction potential if one wishes to compute vibrational frequencies to compare with experiment or if one wishes to use the potentials in Monte Carlo or molecular dynamics simulation calculations.

Sauer and co-workers (ref. 31b) developed such analytical potentials for the water-silica interaction system. The method makes use of the importance of the molecular electrostatic potential (MEP) and uses the functional form of EPEN/2 (empirical potential based on interactions of electrons and nuclei (ref. 38)).

EPEN/2 potential functions V consist of a point charge interaction term V^{point} and a term $V^{n.\ spec.}$ which involves Buckingham-type potentials (e.g. eq. II.1) for describing non-specific interactions:

$$\Phi = \Phi^{point} + \Phi^{n.spec.} \qquad \text{(III.4)}$$

The Coulòmb interaction term Φ^{point} is computed between molecules that have non-coinciding positions of total electron charges and nuclear charges, the so-called multisite point charge model. The distribution of charges is chosen such that multipole moments or MEP curves are fitted.

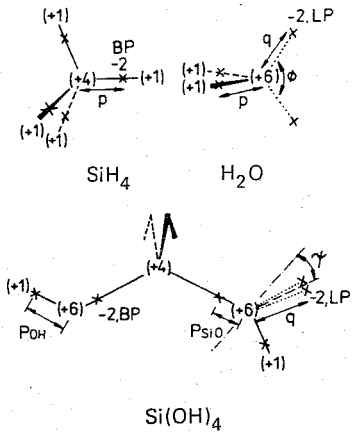

Fig. 1. Point charge models.

An example of such a charge distribution for $Si(OH)_4$ is given in Figure 1. $\Phi^{n.spec.}$ is computed between the total electron charges. Parameters in the potentials are evaluated by fitting quantum-chemical Hartree-Fock interaction energies for a sufficiently large number of relative positions of the interacting molecules. Note that in the procedure applied no basis set superposition error or a Van der Waals energy correction has been made.

In a series of papers Kiselev among others (ref. 39) developed a molecular statistical approach to the adsorption of hydrocarbons in zeolites. The potential was empirically determined, but the zeolite was not approximated by a cluster. The interaction between the hydrocarbon and zeolite lattice was written in terms of atom-atom interactions. The interaction potential of each atom with the zeolite was written as:

$$\Phi_k = -\Sigma_i\, C_i^{(k)}\, \Sigma_j\, r_{ijk}^{-6} + \Sigma_i\, B_i^{(k)}\, \Sigma_j\, r_{ijk}^{-12} - \alpha^{(k)} E^2(r)/2 \qquad \text{(III.5)}$$

In case adsorption of polar molecules is considered the corresponding contributions of the orientation electrostatic interactions of dipole and quadrupole moments of the whole molecule with the zeolite lattice ions have to be added to the total molecule potential. In eq. (III.5) r_{ijk} is the distance between the centre of the k^{th} atom and j^{th} ion of type i, $C_i^{(k)}$ and $B_i^{(k)}$ are the constants for interaction between the k^{th} atom of the molecule and the lattice ion of type i, $\alpha^{(k)}$ is the polarisability of C or H atoms, and E(r) is the resulting electrostatic field at position r inside the cavity (i.e. at the centre of the atom k of the molecule). The summation was carried out over all j ions of each type i inside the chosen region of the lattice.

The constants $C_i^{(k)}$ were not calculated using the London formula (III.3), but from the Kirkwood-Muller formula (ref. 40):

$$C_i^{(k)} = -6mc^2 \, \alpha_i\alpha_k \, / \, (\, \alpha_i/X_i + \alpha_k/X_k \,) \qquad \text{(III.6)}$$

where α_i and α_k are the polarisabilities and X_i and X_k are the magnetic susceptibilities of atoms i and k, respectively, m is the mass of the electron, and c is the velocity of light. From the work of Hotza and Zahradnik it appears that expression (III.3) should be preferred.

The constants $B_i^{(k)}$ were empirically determined from the potential minimum of the pair interaction of an isolated lattice ion of type i having a charge q_i with an atom of type k of the hydrocarbon:

$$B_i^{(k)} = 1/2 \, r_o^6 \, (\, C_i^{(k)} + 1/3 \, q_i^2 \alpha^{(k)} r_o^2 \,) \qquad \text{(III.7)}$$

It is assumed that the equilibrium distance r_o is equal to the sum of the radius of the i^{th} type ion of the zeolite lattice and the Van der Waals radius of the k^{th} atom of the hydrocarbon.

A rather drastic assumption was made concerning framework atom charges as well as extra framework cation charges. The charges on Si and Al atoms were assumed to be zero; on the oxygen atoms the negative charge required to compensate for positive charge of the extra framework cations was evenly distributed (e.g. for Na-X). Some of the Na charges were +1, others close to +.5 for reasons of symmetry. Notwithstanding this approximation rather good agreement between computed and measured heats of adsorption was found. Applied to adsorption in silicalite a linear relation between isosteric heat of adsorption and mean polarizability of the adsorbed molecule was found. In this case no channel cations are present, so inspection of expressions (III.4) and (III.6) indicates the dependence on $C_i^{(k)}$, which relates to the atom polarizabilities of the molecule.

Recently Kiselev's approach has been adapted to compute the location of pyridine in K-L (ref. 41) and to compute the adsorption geometry of methane in zeolite Y (ref. 42) and also in mordenite and ZSM-5 (ref. 43) as a function of temperature and Al/Si ratio, using Monte Carlo techniques.

The interaction with H_2O was studied by the same approach (ref. 44). Charges in the molecule atoms were determined using quantum-chemical calculations. As the temperature increases one observes a change in molecular distribution from wall adsorbed positions to the middle of the cavity. The H_2O simulations show clustering of the H_2O molecules occluded in wide pores as predicted by Sauer among others (ref. 31).

Again the charges on the framework cations have been assumed to be zero and charge has been smeared out over the oxygen atoms, dependent on Na^+ concentra-

tion. It should be remembered that the parameter $B_i^{(k)}$ depends on this charge, so proper application of Kiselev's expressions requires re-evaluation of the parameters dependent on zeolite compositions. In addition the use of Lennard-Jones-type potentials may be questioned, since, as we discussed, the Buckingham potential appears to be favoured.

Notwithstanding significant understanding and progress in the development of hydrocarbon zeolite lattice potentials, it is also clear that major questions remain unsolved. The question of implementation of quantum-chemically cluster-derived potentials into the zeolite lattice properly accounting for long-range electrostatic interactions has not been studied.

The use of variations of Kiselev's potential makes practical and successful simulations possible.

Application to more general problems requires a more detailed study of the potentials to be used.

The quantum-chemical studies on acidity and interaction between organic molecules and cations in zeolites to be discussed now can be considered to be first approaches to further improvement.

As follows from the introductory part of this section, a study of the formation of hydrogen bridges, the elementary step in Bronsted acid reactions, requires careful consideration of local electrostatic interactions.

The electrostatic potential along the zeolite wall probed at the proton position should give a reasonably accurate value of the bond strength between proton and oxygen. On the basis of this philosophy Goursot, Weber and co-workers (ref. 45) provide MEP maps of clusters containing four tetrahedral units, containing a different ratio of Al and Si atoms modelling the wall of offretite. The computations are of minimal basis STO type or Extended-Huckel. No optimization of distances or angles was attempted.

The MEP determined potential for the proton positioned opposite to an O atom bridging an Si and Al atom showed a significant increase from -221 kcal/mol to -276 kcal/mol upon comparing two four-tetrahedra string, one with one Si replaced by Al and the other with two Si atoms replaced Al. This additional aluminium substitution increased the negative charge on the oxygen atoms.

This result agrees with the experimental observations (ref. 46) that the intrinsic acidity per Bronsted acid site decreases with increasing lattice Al/Si ratio.

Earlier semi-empirical calculations (ref. 46a) also indicated the increased bond strength of the

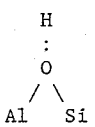

bond if the Si tetrahedron becomes coordinated to tetrahedra with Al as cation. The larger degree of electron donation possible for Al compared to Si, in these calculations again give a higher oxygen charge, increasing the proton–oxygen interaction.

Using

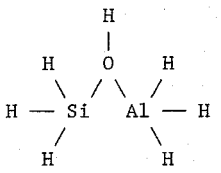

clusters, Mortier, Sauer among others (ref. 47) demonstrated the significant weakening of the OH bond in the bridging configuration compared to end-on-bonded OH. With ab-initio calculations and optimized cluster geometries they observed a decrease between bridging and end-bonded OH of 200 kJ/gat H using a reasonable quality basis set. Compared to the non-protonated cluster, the Al–O and Si–O bond lengths appeared to be considerably longer (δr_{Al-O} = 0.12 A, δr_{Si-O} = 0.09 A).

Sauer (ref. 31d) also computed the interaction energies of H_2O with such clusters. Whereas the interaction of water with siloxane is only 10.1 kJ/mol, it increases to 58.4 kJ/mol for bridging hydroxyl in the Al-Si cluster. The interaction with terminal hydroxyl in a comparable calculation gave 16.4 kJ/mol stabilization.

O'Malley and Dwyer (ref. 48) found a decrease in OH frequency when comparing the proton on the bridging oxygen of the Al–Si containing dimer with end-on hydroxyl.

These results indicate that at least qualitatively correct trends on Bronsted acidity can be derived from cluster ab-initio calculations.

Allavena (ref. 49) extended the clusters so that they were terminated with OH groups instead of H atoms and Van Santen et al. (ref. 50) studied three- and four-tetrahedra-containing rings in which one Si atom was replaced by Al. Both groups used ab-initio methods using varying basis sets. The effect of proton attachment versus compensating Na^+ ions on fully geometry-optimized clusters was studied (ref. 50). As earlier observed by Mortier et al. (ref. 47) significant changes in angle and distance are found. The high Bronsted acidity of a proton attached to a bridging O-atom was confirmed. The conformational changes found for geometry-optimized clusters indicate that the studies should be extended so that geometry constraints due to the embedding of the cluster in the zeolite lattice can be evaluated.

Allavena (ref. 49) and Catlow (ref. 50) also considered the embedding problems of clusters in an electrostatic field. The electrostatic potential on

the cluster atoms contained a Madelung potential correction simulating its value in an extended zeolite lattice. Large changes in hydrogen bonding are observed in the presence and absence of such a Madelung field. It is currently unclear whether the approximate nature of the cluster models (negatively charged, or OH- or H-terminated, limited basis set) requires embedding in an effective electrostatic field or what charges should be used on the atoms modelling the zeolite lattice.

Although semi-empirical calculations (refs. 29, 46a, 51) have provided new insights into the physics of zeolite acidity, it appears that ab-initio calculations are required to enable the prediction of the detailed behaviour of molecules that become protonated. One of the main reasons is the high-quality requirement of the computed local electrostatic interactions.

Few quantum-chemical studies are available on the interaction of cations or metal atoms with a cluster modelling the zeolite framework. Sauer et al. (ref. 30) studied the interaction of Ni^{2+} and Mg^{2+} with

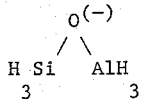

clusters. They found that this interaction is well described with a point charge model. The computed O-M equilibrium distances are $\approx$ 1.85 Å. They estimate the interaction with an Ni atom to be weak and not larger than 30-50 kJ/mol.

There exists a semi-empirical calculation of ethylene interacting with a Na^+ ion attached to an alumino-silicate ring (ref. 31c). However, no ab-initio studies are available to confirm the result that the presence of the alumino-silicate ring significantly alters the binding geometry of adsorbed ethylene.

On the basis of the analysis of bonding in zeolites presented in Sections II and III we recommend the following strategy to derive zeolite-adsorbate interaction energies and geometries.

Quantum-chemical cluster calculations having a geometry representative of the complex geometry to be studied should be done to derive EPEN/2 potentials between cluster and adsorbate. In case proton transfer is studied, also the potentials between framework atoms should also be modelled.

In an independent study atom-atom potentials between lattice atoms at a distance equal to two or three atom-atom distances from the adsorption site have to be established along the lines outlined in Section II. Effective framework atom charges can be derived from quantum-chemical cluster calculations. The dielectric constant $\epsilon(\infty)$ may be estimated from the Clausius-Masotti relation using atom polarizabilities corrected as discussed for the computation of

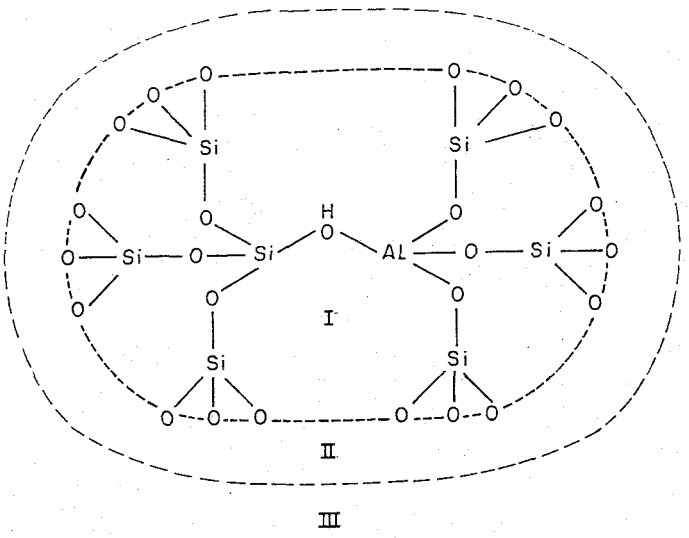

Fig. 2. Division of space around a reactive zeolite site.

the London interaction (ref. 20). These are the ingredients required for the following approach.

As illustrated in Figure 2, we have divided the space around the adsorption complex in three regions. In region I all interactions are described in terms of EPEN/2-type potential functions. Covalent bonding between atoms in region I and II can be described using potentials derived from the undisturbed lattice potential study; the same holds for covalent bonding between atoms in regions II and III.

Whereas the atom positions in region III are to remain fixed and are to be the same as in the undisturbed lattice study, relaxation of atom-atom distances is allowed to occur in regions I and II.

The electrostatic contribution to the potentials between the atoms in region I and that in regions II and III as well as between the atoms in region II and between the atoms of region II and III are computed using expressions such as:

$$\Phi(\text{coul})_{ij}^{IJ} = 1/\epsilon(\infty)\ q_i q_j / r_{ij}$$

$\Phi(\text{coul})_{ij}^{IJ}$ describes the Coulomb interaction between atoms in regions I and J. Atom i is located in region I and atom j in region J. q_i and q_j are their respective charges.

Although for different systems part of this scheme has been accomplished and as we discussed the techniques are in principle available, no complete study along the lines sketched is available yet.

IV. COMPUTER MODELLING TECHNIQUES

Introduction

Computer Aided Molecular Modelling or CAMM has become a well-established tool in organic chemistry within a time span of 10 years. An important application area is in the field of macromolecules, for example the design of new drug molecules by pharmaceutical industries (ref. 52). CAMM, a combination of computational chemistry and molecular graphics, has almost bridged the gap between theoretical and experimental chemistry. On the one hand, the 'workbench chemist' now has access to the insight gained by theory through his CAMM facility, aiding him to interpret his findings and moreover to select the most promising experiments in advance. On the other hand, the theoretical chemist now has a very natural graphical interface to his computational routines. Both share the benefits of an easily gained insight into the three-dimensional structure of molecules and related properties, and a better mutual communication.

In molecular modelling a wide range of computational methods is available in an integrated way (ref. 53). Many problems can adequately be tackled with empirical techniques such as molecular mechanics (ref. 54) and molecular dynamics (ref. 55), the first mainly to find the conformation of molecules and the latter to simulate the behaviour. A bottleneck often still is the availability of good atom-atom force fields, especially for metals and other 'non-organic' elements. Molecular orbital routines and even ab-initio programs (ref. 56) are also part of a standard CAMM facility. Next to this, experimental data, in the form of crystallographic databases such as the Cambridge Structural Database, and empirical search techniques applying QSAR (Quantitative Structure Activity Relationships) (ref. 57) are important ingredients.

The possibilities will be sketched to adapt and extend the techniques of CAMM, whose merits and influence have perhaps been slightly exaggerated for clarity in the first paragraph, to zeolite chemistry (ref. 58). Another source for techniques in zeolite modelling is (inorganic) crystallography, a field where graphics has already been applied for many years (ref. 59). To this end the available hardware and software, including the techniques of CAMM, will be discussed before we focus on applications in our field. Although zeolite modelling also gains its strength from combining existing computational and experimental approaches with dedicated three-dimensional graphics, we will mainly cover the latter in the present chapter.

Hardware

The developments in CAMM have hitherto clearly been hardware driven, but this situation seems to change in favour of software developments. The reason is that, from a technological point of view, for the hardware a plateau is

being approached which offers graphics of sufficient quality. The prices for this hardware will continue to drop because there is now a sound competition and the emergence of software standards (UNIX, PHIGS) will make it easier to change systems. Software has not been able to keep pace with the hardware developments, but may be able to catch up during the plateau period mentioned

The whole field of interactive three-dimensional graphics was opened up by the Evans & Sutherland PS300 family of terminals, which was introduced in the early eighties. The concept of dedicated and very fast hardware, addressing a 'vector display', to manipulate wireframe models was the important innovation. Structures, once loaded from a host computer, could be rotated, translated and zoomed in real time by turning dials. Other important facilities are hardware clipping (making parts of the structure invisible), depth cueing (suggesting depth by lowering the intensity of lines further away), perspective and stereo (yielding a realistic 3-D impression with the aid of special spectacles).

Only lines and dots (Figure 3) could be displayed, the latter to create a surface (ref. 60). The advantage of wireframe models is the possibility to look through the structure as opposed to solid models (Figure 5) where one can view only the outer surface of a molecule. The latter display mode will therefore never fully replace the stick models, which are the best way to show chemical structure. Ball-and-stick models, with dotted spheres to represent the atoms, are also very instructive.

The last few years have shown a very rapid development of general purpose super workstations (e.g. from Silicon Graphics or Ardent), which have now even taken the lead in pure graphics performance. Interactive solid rendering, which requires real-time hidden line removal and shading, has now become possible on 'affordable' (k$40-k$200) machines. This is combined with very powerful CPUs (more than 10* VAX-780 performance) which often exhibit a parallel architecture. These are almost ideal CAMM machines because superb graphics can be done on the same computer which performs the computational chemistry calculations. Most of these workstations contain separate graphics processors to do part of the display operations, but nevertheless offer new possibilities to integrate calculations with graphics. Most of these new approaches (ref. 61), e.g. calculating and displaying interaction energies or simulating experiments (Figure 4) at the same time the structure is altered, are still to be explored.

Software

Graphics software dedicated to zeolite modelling is still hardly available, but the large commercial packages for CAMM are showing more and more useful features. Since the development and maintenance of a CAMM package is a major effort (more than 1 million lines of code is no exception), good software is mainly obtainable through commercial suppliers. The prices are of the same

Fig. 3. The framework of ZSM-5, drawn by connecting the metal positions with (purple) lines. The inner surface of the channels is indicated by (yellow) dots, generated with the Connoly routine (ref. 60).

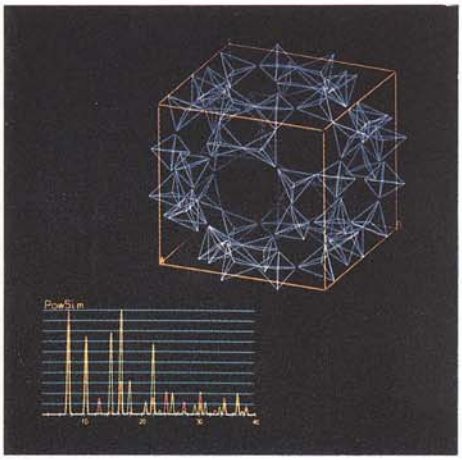

Fig. 4. One unit cell of zeolite A, sketched as tetrahedrons with the program PLUVA (ref. 62). Also given are the diffractograms of the known structure (in red) and the semi-real-time simulation of the displayed, modified structure (in green). With PLUVA the contents of the unit cell can be modelled interactively while the symmetry is conserved. In this demonstration, the tetrahedrons are rotated a few degrees.

Figs. 5a and b. Solid rendering (CPK model) of faujasite, viewing from the large cage into the small sodalite cage (centre of figure a). The crystallographically different oxygen atoms have been given different colours, in order to prove that one of them is inaccessible to pyridine probe molecules as indicated in an infrared experiment. As shown in figure b, the 'yellow' oxygens (identical with the ones in the centre of figure a) are inaccessible for the 'red' pyridine molecule, which can only approach from the large cage.

order as those of the hardware, but considerable discounts are given to academic clients.

A good modelling program is capable of constructing and displaying a molecular or crystallographic structure in various ways, utilising the possibilities offered by modern hardware. Many other possibilities are available, for example quick ways to inquire atom distances, bond angles etc. Zeolite structures are mainly found in the Inorganic Crystal Structural Database (ICSD), but no commercial program offers yet a direct interface to this database as opposed to the organic databases. Molecular mechanics routines to optimise structures, even through an exhaustive search through conformational space, are normally incorporated in the display program. Possibilities to add a solvent or to apply periodic boundary conditions, to simulate a molecule as part of a crystal, are almost standard. The available force fields are optimised for macromolecules and/or small organic molecules, but can be changed by the user. As explained elsewhere in this workshop, force fields for silicalites still need improvement. A molecular dynamics 'engine' also belongs to the standard outfit of a CAMM package, which means a full integration with the graphics. For the simulation of an adsorbate molecule in a zeolite framework (see next section) this implies that the molecule can be followed on the screen while the calculation develops.

Nice interfaces to well-known programs for MO and ab-initio calculations, which are of academic origin, are often offered. This means that the input for these programs can be easily made by constructing the desired molecule and also that the output can be inspected through molecular graphics. For this purpose the program has to be capable of displaying wave functions and charge distributions. This is often done in combination with the display of the Van der Waals surface.

A basic problem with the application of CAMM programs to zeolite, or other inorganic crystals is the fact that the structure is treated as a macromolecule. Only when the crystal is constructed from crystallographic data, at the input stage, is the symmetry taken into consideration. If one wants to modify the structure at a later stage, it is only possible to change the positions of atoms individually (or to re-input a whole new structure). To circumvent this cumbersome procedure, the crystallographic modelling program PLUVA (ref. 62) has been developed. This program incorporates crystallographic symmetry in the display itself by taking advantage of the display capabilities of an Evans & Sutherland PS390 computer. Not only once, but during every display cycle is the crystal constructed by applying symmetry operations on a basic building block (the asymmetric unit). In this way the interactive displacement of one atom results in an immediate modification of the whole structure in such a way that the symmetry is preserved (Figure 5).

Zeolite modelling

As in the case of organic modelling, graphics is an indispensable tool to serve as an interface with energy and other calculations but it also has a value of its own. Gaining insight into the three-D frameworks of zeolites and the possible positions of adsorbates and cations is almost impossible without graphics. For these purposes a standard CAMM program can be very useful (ref. 63). Different display styles can be chosen and cations and organic molecules can be manipulated independent of the zeolite framework. Van der Waals or Conolly routines can be used to create the inner surface of the zeolite. Fitting a molecule in a zeolite pore bears an important resemblance to 'docking' procedures in biochemical applications, for which dedicated tools exist (e.g. distance monitors).

Areas where modelling can play an important role are:

* Modelling of zeolite-adsorbate interactions.
* The search for new zeolite structures.
* Interpretation of diffraction and spectroscopic experiments.
* The search for template molecules and synthesis intermediates.

The first item will be discussed in Section V; the others will only briefly be dealt with in the next paragraphs.

By using symmetry considerations, as attempted by for example by Smith (ref. 64), one can systematically generate geometrically possible zeolite structures. Several other approaches (ref. 65) exist, for example considering possible cage and channel structures, realising that crystals tend to form periodic minimal surfaces (ref. 66). A modelling tool such as PLUVA, capable of rearranging zeolite fragments under crystallographic symmetry limitations and having fast control over the unit cell dimensions, can be of great assistance. Molecular mechanics calculations, such as the approach chosen by Catlow and co-workers (ref. 3), can be used to estimate the stability of a hypothetical structure.

Various analytical techniques are required to investigate the structure of zeolites (X-Ray Diffraction, High Resolution Electron Spectroscopy, Nuclear Magnetic Resonance), acid strength and siting (Infrared spectroscopy) etc. Modelling offers a way to quickly check and interpret the outcomes on a microscopic scale (refs. 67-70), for example to test steric hindering of probe molecules. A fast interface between a crystallographic modelling program and simulation programs (XRD, HREM) is a very powerful tool to elucidate zeolite structures from powder diffractograms (ref. 10). Algorithms which combine crystallographic refinement with molecular dynamics (ref. 71) have, to our knowledge, not yet been tried in this field but they may be as successful as for macromolecules.

Suitable organic molecules, added to the synthesis solution, enhance the selective crystallisation of zeolites. In a number of cases evidence is found

for a template effect, with the molecule exactly filling up the zeolite pores (ref. 72). Molecular modelling tools, including organic databases, are very convenient for searching such molecules. Again the resemblance with biochemical applications, especially drug design, is very strong. Next to this, modelling can be of assistance to unravel the synthesis process, for instance in identifying synthesis intermediates.

V. COMPUTER SIMULATION OF ADSORPTION AND DIFFUSION

The interaction between organic adsorbates and a zeolitic environment plays an important role in the extended field of zeolite science and technology. Directly related to these interactions are adsorption and diffusion phenomena which are thought to have a large impact on the catalytic activity and selectivity of zeolites.

In reactions catalysed by microporous solids, such as zeolites, catalytic selectivity is not only a matter of stoichiometry, but also steric constraints for molecular transport in the zeolite void space can be the reason for the so-called shape selectivity (ref. 73). Shape selectivity can in principle be achieved by adjusting the size (ref. 74) and accessibilities (ref. 75) of the micropores. A distinction is made between three types of shape selectivity depending on whether the pore size limits the entrance of the reacting molecule (reactant selectivity), the departure of the product molecule (product selectivity) or the formation of certain transition states along the reaction coordinate (restricted transition state selectivity).

It will be obvious that the phenomenon of shape selectivity is directly related to adsorption and diffusion characteristics. Since it is difficult to obtain information about these characteristics on a molecular level, especially at elevated temperatures at which the chemical conversions take place, computer simulations might offer alternative approaches to problems encountered in zeolite catalysis research.

In this Section, we will discuss procedures for the description of adsorption and molecular transport phenomena in zeolites. For the simulation of adsorption, the Monte Carlo method is employed, whereas molecular dynamics techniques are used in order to simulate diffusion. In the following sections, we will give a brief overview of the Monte Carlo and molecular dynamics techniques. Finally, both methods will be exemplified by a review of adsorption and diffusion simulation studies of various zeolites reported in the literature.

The Monte Carlo method

The importance of the Monte Carlo method is that it provides us with a tool for calculating macroscopic quantities (energy, temperature, pressure, etc.) of a system for which the intermolecular potentials are known. The reliability of

these calculated properties is therefore determined by the reliability of the intermolecular potentials.

The Monte Carlo algorithm is based on the proposals of Metropolis et al. (ref. 76) and can be characterized by the following three steps:

* give the adsorbate(s) a new configuration (random new position(s) and random new orientation(s)),
* calculate the energy difference between this new configuration and the old configuration: $\delta E = E_{new} - E_{old}$,
* accept this new configuration with a probability proportional to the Boltzmann weight factor at temperature T: $\exp(\delta E/kT)$

These steps are repeated in order to obtain a chain of configurations Γ_i $(i=1,2,\ldots,M)$.

Let us assume we have a system of N particles in a fixed volume V and at a constant temperature T. From statistical mechanics it can be derived that the thermodynamic average of a quantity A can be written as (ref. 77):

$$< A > = (1/Z) \cdot \int d\Gamma \; A(\Gamma).\exp(-E(\Gamma)/kT) \qquad (V.1)$$

where

Γ : the configuration of all particles
(the integration is over all possible configurations)
$E(\Gamma)$: energy of a configuration Γ
$A(\Gamma)$: value of A at configuration Γ
Z : partition function:

$$Z = \int d\Gamma \; \exp(-E(\Gamma)/kT) \qquad (V.2)$$

The purpose of the Monte Carlo method is to calculate the integral as given by equation (V.1) numerically. One (naive) method to achieve this is to generate a set of randomly chosen configurations Γ_i $(i=1,..,M)$. Following this procedure, the average of A can be approximated by:

$$< A > = \frac{\Sigma_{i=1}^{M} A(\Gamma_i).\exp(-E(\Gamma_i)/kT)}{\Sigma_{i=1}^{M} \exp(-E(\Gamma_i)/kT)} \qquad (V.3)$$

However, the statistics of this method will be very poor, because most values of Γ_i will be chosen in a region where $\exp(-E(\Gamma_i)/kT)$ is low (ref. 77).

To circumvent this problem, Metropolis et al. (ref. 76) proposed the method of importance sampling. In this method, the configurations will not be chosen at random but will be selected with a probability $P(\Gamma)$. The average of quantity A for this case can be written as (refs. 76,77):

$$< A > = \frac{\Sigma_{i=1}^{M} A(\Gamma_i) P^{-1}(\Gamma_i) \exp(-E(\Gamma_i)/kT)}{\Sigma_{i}^{M} P^{-1}(\Gamma_i) \exp(-E(\Gamma_i)/kT)} \qquad (V.4)$$

If we choose for the distribution of configurations in the chain the equilibrium distribution $P^{eq}(\Gamma)$:

$$P^{eq}(\Gamma) = \exp(-E(\Gamma)/kT) \qquad (V.5)$$

then we can write for the average of A:

$$< A > = 1/M\Sigma_{i=1}^{M} A(\Gamma_i) \qquad (V.6)$$

Generating a chain of configurations $(\Gamma_1,\ldots,\Gamma_M)$ with a certain distribution can formally be described with the theory of Markov processes (ref. 78). A very important condition to ensure a statistical reliability is that in the course of the simulation it must be possible to reach (in principle) all accessible configurations.

The molecular dynamics method

In this section we will discuss the basic principles of molecular dynamics. Comparisons with Monte Carlo methods will be made in order to highlight the differences and analogies of the two techniques.

As discussed above, Monte Carlo simulations deal with systems which are in equilibrium and so static thermodynamic properties such as heats of adsorption and average siting behaviour can be derived according to equation (V.6).

In a Monte Carlo simulation there is no time scale involved and successive configurations are chosen at random. Molecular dynamics simulations, on the other hand, simulate the time evolution explicitly. So, what you can do with a molecular dynamics simulation is: all one can do with a Monte Carlo procedure, i.e. the evaluation of static thermodynamic properties such as temperature and pressure, but also – and this is of particular interest to us – the determination of diffusivities and site residence times of molecules absorbed in zeolitic pores. These dynamic properties are derived by generating a system trajectory followed by averaging over time. So, for any thermodynamic property A, the average value of A following from a molecular dynamics simulation is given by:

$$<A> = 1/t.\Sigma_{i=1}^{M} A.\delta t_i \qquad (V.7)$$

where M is the number of molecular dynamics sampling points, t is the total simulation time and δt_i is the time step length. Obviously, $\Sigma_{i=1}^{M}\delta t_i = t$. A is the value of property A at a specific time along the trajectory.

Generating a molecular dynamics trajectory is purely based on classical Newtonian mechanics. We consider an ensemble of particles moving in a force

field. The number of particles equals N, the force on particle i (i=1,N) at time t is given by $F_i(t)$, and the position of the particle at time t is represented by $r_i(t)$. A Taylor expansion of $r_i(t)$ around t (until second order) results in:

$$r_i(t+\delta t) = r_i(t) + (dr_i(t)/dt)_t.\delta t + 1/2(d^2r_i(t)/dt^2)_t.(\delta t)^2 \qquad (V.8)$$

$$r_i(t-\delta t) = r_i(t) - (dr_i(t)/dt)_t.\delta t + 1/2(d^2r_i(t)/dt^2)_t.(\delta t)^2 \qquad (V.9)$$

Combination of equations (V.8) and (V.9) yields:

$$r_i(t+\delta t) = 2r_i(t) - r_i(t-\delta t) + (d^2r_i(t)/dt^2)_t.(\delta t)^2$$

$$= 2r_i(t) - r_i(t-\delta t) + (F_i(t)/m_i).(\delta t)^2 \qquad (V.10)$$

and

$$(dr_i(t)/dt)_t = (r_i(t+\delta t) - r_i(t-\delta t)) / 2\delta t = v_i(t) \qquad (V.11)$$

where m_i is the mass of particle i and $v_i(t)$ its velocity at time t.

Equation (V.10) clearly shows that, given the forces on the particles, one is able to generate a trajectory in time without using any knowledge about the particle velocities. However, determination of the velocities might be useful for the evaluation of the particle ensemble temperature from the kinetic energy of the system:

$$E_{kin}(t) = 1/2\Sigma_{i=1}^{N} m_i.v_i^2(t) \qquad (V.12)$$

and hence

$$T(t) = (2/3Nk).E_{kin} = (1/3Nk)\Sigma_{i=1}^{N} m_i.v_i^2(t) \qquad (V.13)$$

wherein k is the Boltzmann constant.

Equations (V.10) through (V.13) define the body of a molecular dynamics algorithm. From equation (V.13) it is obvious that the temperature of the particle ensemble is not constant but fluctuates around the average temperature and hence the kinetic energy of the system is not constant either. It should be noted however, that the total energy, E_{tot}, is conserved throughout the simulation. The total energy is given by:

$$E_{tot} = E_{pot} + E_{kin} \qquad (V.14)$$

where the potential energy, E_{pot}, is related to the force via

$$F = -dE_{pot}/dr \qquad (V.15)$$

Such an algorithm is referred to as an NVE algorithm (constant number of particles, constant volume, constant total energy) (ref. 79). The simulation temperature, T_s, in an NVE simulation can be determined afterwards by integrating over the time:

$$T_s = 1/t.\int T(t)dt \qquad (V.16)$$

The NVE algorithm is employed in cases where the conservation of the total energy is required, that is, when the microcanonical (NVE) ensemble has to be sampled. However, in most practical processes, i.e. isothermic ones, a constant temperature is required. In these cases, one samples the canonical ensemble and one needs to employ an NVT algorithm (constant number of particles, constant volume, constant temperature). This algorithm is basically the same as the NVE algorithm but a temperature correction step is incorporated in order to ensure a constant temperature. Equation (V.10) is used to predict the new positions of the particles. Equations (V.11) and (V.13) are used to calculate the temperature T(t) of the ensemble. Let $T_w(t)=T_w$ be the desired simulation temperature, then

$$T_w = (T_w/T(t)).T(t) \qquad (V.17)$$

and so with the use of equation (V.13):

$$T_w = (T_w/T(t)).(1/3Nk)\Sigma_{i=1}^{N} m_i.v_i^2(t)$$

$$= (1/3Nk)\Sigma_{i=1}^{N} m_i(v_i(t).(T_w/T(t))^{1/2})^2 \qquad (V.18)$$

From equation (V.18) it follows that the velocities of the particles at time t need to be scaled by a factor $(T_w/T(t))^{1/2}$ in order to maintain a constant temperature. With these scaled velocities and the forces on the particles, the new (corrected) positions of the particles are calculated via:

$$v'_i(t) = (T_w/T)^{1/2} \cdot v_i(t) \qquad (V.19)$$

$$r_i(t+\delta t) = r_i(t) + v'_i(t).\delta t \qquad (V.20)$$

Basically, the implications of equations (V.17) and (V.18) are that the surroundings of the system under consideration are regarded as a medium with an infinite heat capacity (isothermic bath). All heat which is added to, or withdrawn from, the system comes from, or goes to, the isothermic bath. If we regard simulation of diffusion of adsorbates in zeolites, the NVT algorithm is based on the assumption of an infinite coupling between the adsorbates ensemble temperature and the zeolite energy content. On the other hand, the NVE algorithm assumes no coupling of this kind at all.

An advantage of the NVT algorithm over the NVE algorithm is that the NVT algorithm is cheaper in computer time. This is due to the fact that in the NVE algorithm the ensemble has to be equilibrated for a rather long time to establish a constant total energy which does not fluctuate too much as a result of simulation start-up effects. Furthermore, it seems logical that the zeolite lattice is influenced by the temperature of the adsorbates ensemble, so the NVT algorithm will reflect the physical reality in a better way.

Simulation of adsorption and diffusion; models

In the Monte Carlo adsorption simulations the following approximations are used:

* no adsorbate-adsorbate interactions are considered, so all calculations correspond to low coverage of adsorbate molecules.
  However, in a section to come, we will also meet studies in which the adsorbate-adsorbate interactions are not neglected and hence adsorption phenomena apart from the zero filling area are examined.
* the zeolite lattice is rigid
* the adsorbate molecule is rigid.

With these assumptions, the potentials contain only adsorbate-zeolite interactions which can be approximated by a pairwise potential Φ_{ij} (ref. 39d). Thus the average potential energy for a given configuration Γ is given by:

$$\langle E_{pot} \rangle_\Gamma = \Sigma_{ij} \Phi_{ij} \qquad (V.21)$$

where i and j run over all the atoms in the zeolite and adsorbate, respectively. The potential Φ_{ij} is usually a combination of a (6-12) Lennard-Jones part and a coulombic part. The adsorption enthalpy following from a Monte Carlo simulation follows from averaging over all configurations that are generated during the simulation (eq. V.6):

$$\langle Q_s \rangle = 1/M \; \Sigma_{i=1}^{M} A(\Gamma_i) \qquad (V.22)$$

In order to eliminate the effect of unit cell boundaries, periodic boundary conditions are used. To save computer time, the potentials are truncated at a cut off radius which is of the order of the size of one unit cell. To make an estimate of the statistical reliability, the simulation can be divided into subruns of 10,000 Monte Carlo steps each. The standard deviation of the interaction energy (eq. V.22) can then be calculated from these subruns. One single run takes from ten up to twenty subruns.

Just as with the Monte Carlo simulations, with the molecular dynamics simulations both the adsorbate and the zeolite lattice have so far been assumed to be rigid. However, adsorbate-adsorbate interactions are not neglected, so the

potential energy of adsorbate i can be represented by:

$$E_{pot,i} = \Sigma_r \Phi^{(1)}_{r,i} + \Sigma_{j<>i} \Phi^{(2)}_{i,j} \qquad (V.23)$$

where r runs over all the atoms in the zeolite lattice and j runs over all the adsorbates except adsorbate i. $\Phi^{(1)}$ is the adsorbate-zeolite interaction (a combined Lennard-Jones/coulombic interaction) and $\Phi^{(2)}$ is the adsorbate-adsorbate interaction (purely Lennard-Jones). The total average potential energy of the ensemble at a specific time i out of the trajectory is given by:

$$<E_{pot}>_i = 1/N \Sigma^N_{i=1}\{ \Sigma_r \Phi^{(1)}_{r,i} + 1/2 \Sigma_{j<>i} \Phi^{(2)}_{i,j} \} \qquad (V.24)$$

with N the number of adsorbates in the zeolite. The factor 1/2 is introduced to avoid double counting.

From equation (V.23) and with the use of equation (V.15), an expression for the force on particle i can easily be derived:

$$F_i(t) = -d/dr \{ \Sigma_r \Phi^{(1)}_{r,i} + \Sigma_{j<>i} \Phi^{(2)}_{i,j} \} \qquad (V.25)$$

Note that $F_i(t)$ is a function of the time because $\Phi^{(1)}$ and $\Phi^{(2)}$ are time-dependent. Note also that $F_i(t)$ is a vector, whereas $E_{pot,i}$ is a scalar. Equation (V.25) defines a force field for molecules migrating in the pores of a zeolite. This force field can be used directly in the MD algorithms as discussed in the previous section to generate a system trajectory in time. From this trajectory, diffusivities are easily calculated via the Einstein relation (ref. 80):

$$D = 1/6 <r^2>/t \qquad (V.26)$$

where $<r^2>$ is the mean square distance travelled by the adsorbate molecules during a period t.

Adsorption enthalpies (Q_s) are calculated by using equation (V.7):

$$<Q_s> = 1/t \Sigma^M_{i=1}<E_{pot}>_i \cdot \delta t_i \qquad (V.27)$$

where $<E_{pot}>_i$ is given by equation (V.24), M is the number of time steps taken for the simulation, and δt_i is the time step length.

Discussion of computer simulation studies

Computer simulations of adsorption and diffusion in zeolites have gained much interest over the last few years. This increasing interest is probably due to the possibilities that modern computer hardware and methods developed in computational chemistry offer to zeolite catalysis research. The number of papers devoted to computer simulation of adsorption and diffusion which have appeared in the literature from the early 80's to 1988 has increased considerably compared to the foregoing years.

In this section, we intend to discuss several studies which have recently appeared in the literature. In the first instance, we will restrict ourselves to studies which are based on the theory as outlined in Section V. However, some attention will also be paid to other (computer) simulation studies.

Leherte et al. (ref. 44) extensively studied water adsorption in a ferrierite-type zeolite structure. The zeolite-water potential was a combined Lennard-Jones/coulomb potential, whereas the water-water potential was derived from Matsuoka et al. (ref. 81). They did not use the zero-filling approximation but considered a varying water occupancy of the zeolite. The amount of water adsorbed varied from 5.88 up to 11.95 molecules per unit cell (total number of adsorbates considered: N=40-80). Using Monte Carlo simulations, they were able to calculate water adsorption enthalpies which were in reasonable agreement with experimental data. Furthermore, they studied the configurations of the adsorbed water molecules. It was found that the water molecules tend to form cage structures in the zeolite cavities and remain far from the centre and the walls of the 10-membered ring channel. However, in the 8-membered ring

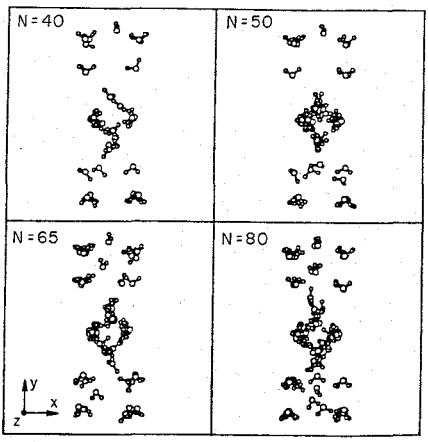

Fig. 6. Plots of one significant configuration for all water molecules corresponding to each density: (a) N=40, (b) N=50, (c) N=65 and (d) N=80. (Figure taken from reference 44).

channels, the molecules are closer to the walls. Figure 6 shows a plot of one significant configuration for four different densities. In these plots, the clustering of the water molecules is clearly demonstrated.

Yashonath et al. (ref. 42) simulated methane adsorption in zeolite Na-Y using a Monte Carlo technique and a Lennard-Jones/coulomb zeolite-adsorbate interaction potential. Apart from the calculation, they paid special attention to the temperature dependency of the adsorption process. Using the zero-filling

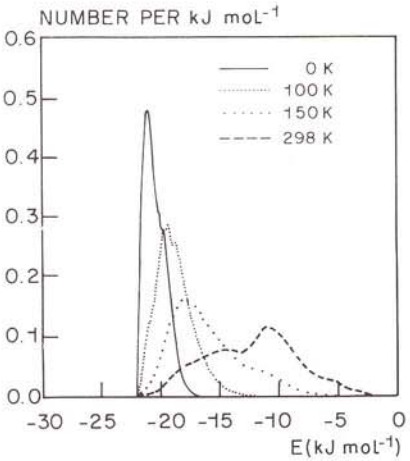

Fig. 7. Plots of the distribution functions of the potential energy of interaction of methane with zeolite Na-Y at different temperatures. (Figure taken from reference 42).

approximation, they generated so-called potential energy distribution functions (PEDF) which relate the potential energy of a configuration to the fraction of adsorbed molecules being in that particular configuration. Figure 7 displays a PEDF at different temperatures for methane in zeolite Na-Y.

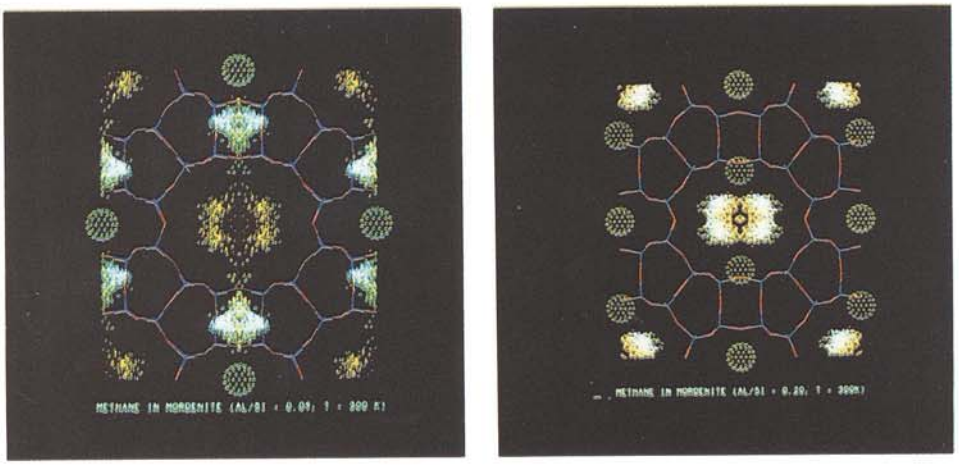

Fig. 8. Distribution of methane adsorbed in mordenite at 300 K and Al/Si=0.09 (a) and Al/Si=0.2 (b) as obtained by Monte Carlo calculations. The zeolite structure is represented by rods and the sodium ions by spheres. Each spot inside the zeolite pore represents the projection of the centre of mass of the methane molecule. (Figure taken from reference 43).

A similar Monte Carlo study was carried out by Smit et al. (ref. 43), who studied methane adsorption in the zeolites silicalite, Na-Y and Na-mordenite using the same potentials as Yashonath et al. (ref. 42). For the case of Na-mordenite, special attention was paid to the influence of the zeolitic Al/Si ratio on the adsorption process. It was found that the side-pockets, situated at the edges of the 12-membered ring channels are strong adsorption sites for methane. By increasing the Al/Si ratio, and thus increasing the sodium content, these side-pockets are gradually blocked by sodium ions. This feature results in totally different adsorption characteristics, as can be seen in Figure 8. In this figure, the dots represent the centre of mass of the methane molecule adsorbed in the mordenite pores. At low Al/Si ratios (Figure 8a) methane is preferentially adsorbed in the side-pockets (high density of dots) whereas at higher Al/Si ratios these side-pockets are blocked with sodium ions. This pore-blocking feature is more quantitatively expressed in the PEDF in Figure 9, where one adsorption site disappears with increasing Al/Si ratio.

In line with the water-adsorption Monte Carlo simulations, Leherte et al. (ref. 82) studied the diffusivity of water adsorbed in ferrierite. Using molecular dynamics techniques and the same potentials as used in their Monte Carlo study on the same system (ref. 44), they calculated the self-diffusion coefficient of water using the Einstein relation (eq. V.26). By plotting the mean square distance travelled by the water molecules against time, the diffusion coefficient was found to be 0.5×10^{-9} m^2/s. Figure 10 displays such a plot for the three different directions x (crystallographic a-axis), y (b-axis) and z (c-axis) as well as for the average displacement. In ferrierite, only a displacement in the y- and z-directions is observed due to the fact that along the x-axis the ferrierite channels are not connected. Thus, there is no way for the molecules to move from one channel to another following that direction and consequently their mobility is lowered.

Yashonath et al. (ref. 83) introduced site residence times (τ_s) and cage residence times (τ_c). They performed molecular dynamics simulations of methane self-diffusion in zeolite Na-Y using the same potentials as in their earlier Monte Carlo study on the same system (ref. 42). From these simulations, they were able to estimate the average residence times of methane molecules at adsorption sites and in the supercages of the faujasite structure. Figure 11 displays their results. At temperatures above 200 K, the mobility of the methane molecules increases considerably. It is also observed that site residence times are nearly negligible at temperatures higher than 150 K. Furthermore, the average residence time for a methane molecule in a supercage is estimated to be 2-3 ps at room temperature.

Diffusivities of methane in various all-silica zeolites, using molecular dynamics approaches, were studied by Den Ouden et al. (ref. 84). In their

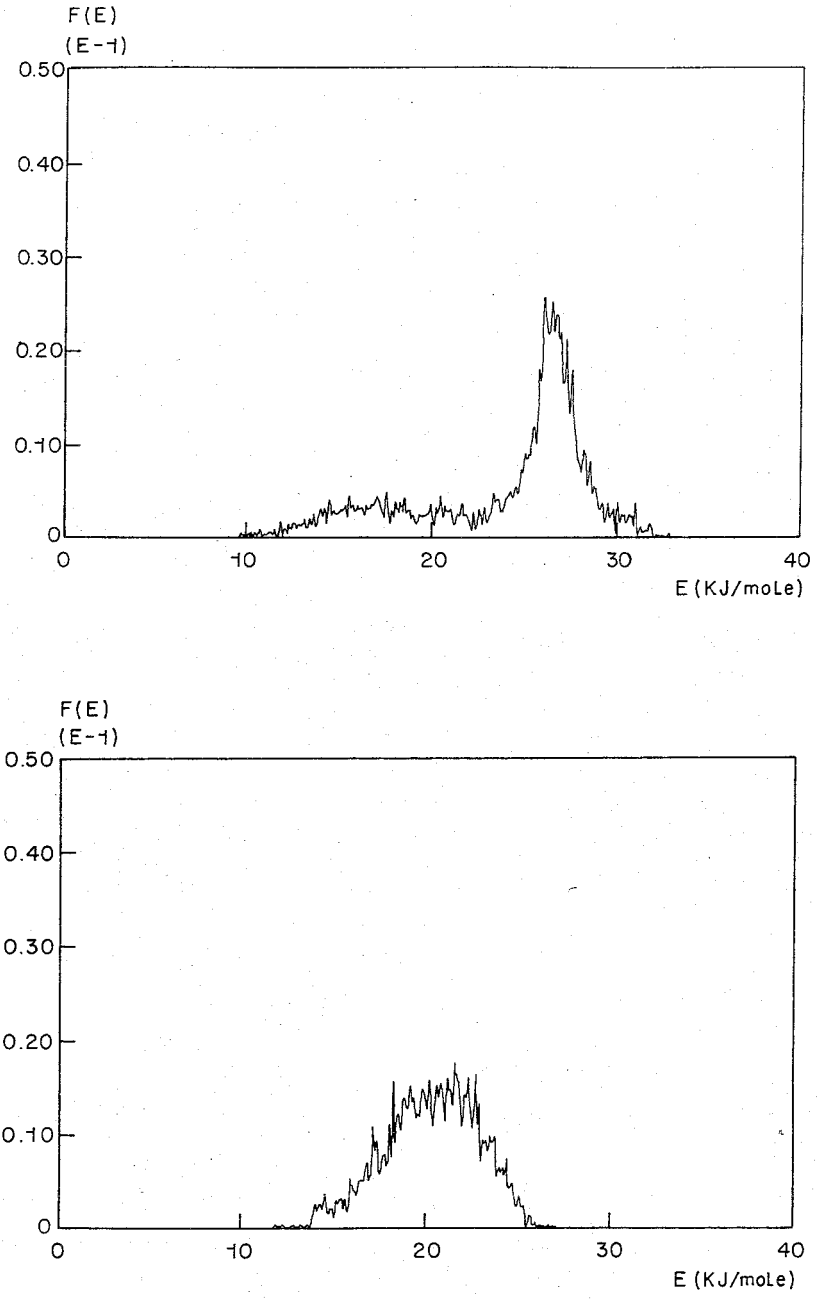

Fig. 9. Plots of the distribution functions of the potential energy of interaction of methane with zeolite Na-mordenite at different Al/Si ratios. For low Al/Si ratios (a, Al/Si=0.09), two distinct adsorption sites can be appointed. For high Al/Si ratios (b, Al/Si=0.20), only one adsorption site is left.

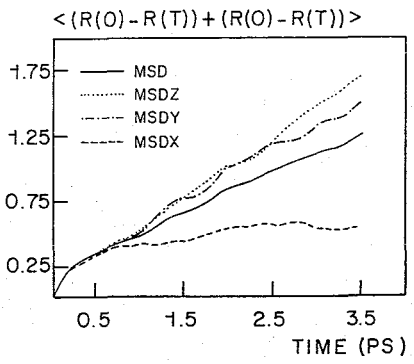

Fig. 10. Mean square deviation of the positions of the water molecules along the x-axis, y-axis and z-axis. The x, y and z directions are associated with the a, b and c cell parameters, respectively. (Figure taken from reference 82).

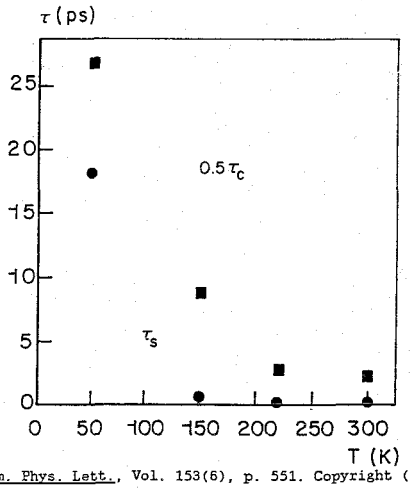

Fig. 11. Temperature dependency of the site (τ_s, dots) and cage (τ_c, squares) residence times for methane in zeolite Na-Y at a loading of six molecules per supercage. Statistical uncertainties are of order 20% for the three highest temperature points and at least twice as large for the lowest temperature. (Figure taken from reference 83).

study, special attention was paid to the influence of the zeolite topology on the diffusion process. Site residence times for methane migrating in the micropores of the zeolites silicalite and mordenite were visualised by using computer graphics. Figure 12 displays trajectories for one methane molecule migrating in the pores of mordenite and silicalite, respectively. The force field in which the molecule moves is caused by the presence of the zeolite

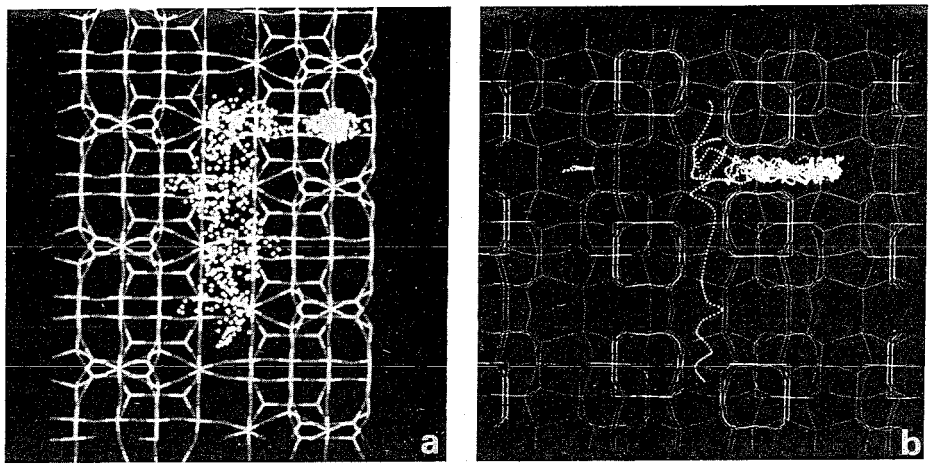

Fig. 12. Trajectory of a methane molecule migrating in mordenite (a) and silicalite (b) over a time period of 100 ps. The zeolite structure is represented by rods. The dots represent the position of the methane molecule at subsequent time intervals. For mordenite (a), the main channel is vertically displayed and the zeolite loading is two molecules/unit cell. The straight channel for silicalite (b) is vertically displayed, the sinusoidal channel horizontally. The zeolite loading is four molecules/unit cell. Both simulations were carried out using an NVT algorithm at T=300K. (Figure taken from reference 84).

lattice and the other methane molecules (not displayed in the figure). Obviously, the side pockets in mordenite (Figure 12a) are adsorption sites with a relatively long residence time (high density of dots). The same is true for methane migrating in the sinusoidal channels in silicalite (vertically displayed in Figure 12b), in which the methane molecule resides much longer than in the straight channels.

Only very recently, June et al. (ref. 85) reported a study on statistical mechanics and molecular dynamics for the modeling of sorption and transport of hydrocarbons in pentasil zeolites. Statistical mechanical relations have been employed for the determination of Henry's constants, isosteric adsorption enthalpies and adsorbate conformational properties for butane and some hexane isomers. Furthermore, molecular dynamics simulations have been employed for the determination of the self diffusivity of various hydrocarbons in silicalite.

A diffusion study based on a Monte Carlo approach was carried out by Palekar et al. (ref. 86) and Pitale et al. (ref. 87). With their approach, they simulated gravimetry experiments and tracer diffusion. They were able to establish the relation between the variation of diffusivity and sorbate concentration as obtained by experiment.

Finally, a very elegant adsorption/diffusion model which is not based on any of the methods discussed in the previous sections was developed by Derouane et al. (refs. 88,89,90). In this model, the curvature of the adsorption surface is taken into account, and it enables one to find analytical expressions for the van der Waals interaction energy and the corresponding force on the adsorbate. With this model, one is able to compare adsorption characteristics in microporous solids with adsorption on flat surfaces. Figure 13 plots the activation

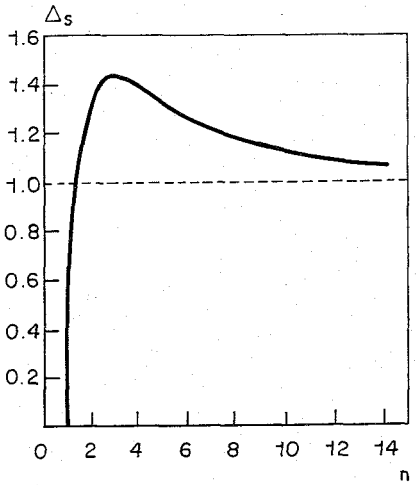

Fig. 13. Relative activation energy, δ_s, for promoting a molecule from the pore wall to the centre of the cavity as a function of the cavity size n (units of r_m). (Figure taken from reference 88).

energy δ_s needed to promote a molecule from the pore wall to the centre of the cavity as a function of the cavity size (in units of n times the adsorbate radius, r_m). δ_s is a parameter accounting for surface curvature effects that may be regarded as a relative (to the flat surface case) activation energy. Obviously, for n=1, the adsorbate radius equals the cavity radius resulting in a maximum van der Waals attraction and hence yielding a zero (sticking-) force acting on the adsorbate. This case is referred to as the floating molecule state. For $n \geq 1.5$, the activation energy always exceeds the flat surface activation energy. Hence, adsorbates in zeolites tend to be more sticked to the internal micropore surface than in the case of adsorption on a flat surface. In this respect, diffusion of small adsorbates at moderate temperatures can be seen as a hopping over the corrugation barriers of the pore wall rather than colliding with the wall and being reflected. Diffusion of chain molecules at moderate temperatures will appear as a creeping motion along the zeolite micropore walls which is referred to as creep diffusion.

From the above discussed studies, two main conclusions on Monte Carlo simulations of adsorption emerge. First of all, using empirical potentials, the agreement of the calculated adsorption enthalpies with experimental data is reasonable indicating a proper description of the adsorbate–zeolite and adsorbate–adsorbate interaction with respect to the particular properties studied. It should be stressed however, that little work has been done on systems with variations in the zeolitic Al/Si ratio. More extensive research in the area of these potentials is certainly necessary. Bezus et al. (ref. 39a) and Kiselev et al. (refs. 39a,b,c) already developed potentials for this case both for organic and inorganic adsorbates.

Secondly, Monte Carlo simulations allow us to study adsorption on a molecular level. This detailed information can be considered as very valuable in zeolite catalysis research. However, the Monte Carlo studies carried out so far deal with rather small systems which are not of primary interest to catalysis research. Recent studies on larger molecules indicate that an extension of these (preliminary) studies to larger adsorbates is possible (ref. 85).

Finally, a promising future application of Molecular Dynamics techniques is in the field of zeolite synthesis. Since the study of zeolites or zeolite precursors in contact with the synthesis mother liquor in the presence or absence of organic template molecules is hard to access by direct experiments, Molecular Dynamics studies might offer a powerful approach to this problem.

Molecular dynamics simulations are indispensable techniques to understand mass transport and chemical dynamics in porous solids on a molecular level. Whereas applications to the computation of mass transport properties have appeared, the development of studies on transition dynamics to determine chemical reaction rates requires the development of potential energy surfaces by methods as discussed in Section II.

VI. FUTURE PERSPECTIVES

Zeolite science currently is an active field for the development of modelling techniques useful in solid state chemistry applications.

Because the potentials to be used have still not completely been determined and a few basic questions remain to be solved, it is also a subject of interest to theoretical physical chemistry.

The question of the relative importance of long range electrostatic interactions versus short range interactions cannot be considered to be definitely solved. It may be expected that application of quantumchemical techniques and the increasing computerpower that is becoming available will soon produce the potentials required to study systematically the packing of molecules in the micropores of the zeolite.

The Monte Carlo method is suitable to approach this problem important for zeolite-synthesis and the physical chemistry of cation exchange. Molecular dynamics in combination with vibrationspectroscopy will provide a sensitive test on the potentials used, by computation of dynamic properties.

In order to provide a basis to the many reaction mechanisms postulated to occur in zeolites the relative stability and potential energies of proposed transition states will have to be evaluated. This requires a solution of the problems of hydrogen bonding in zeolites. In view of the high accuracy of the computations required for the time being this problem can be best approached by studying small model clusters.

The indication that zeolite acidity is mainly determined by short range interactions provides avenues for chemical manipulation of Bronsted acidity and will make this a field of intensive experimental as well as theoretical research.

Successes of the current states of zeolite theory are the prediction and its experimental confirmation of cation positions in high Al-content zeolites as well as the predicted and experimentally confirmed small difference in cohesive energy of siliceous zeolites.

Quantum chemical cluster calculations appear to simulate trends in zeolite acidity quite well, if one changes zeolite composition.

Monte Carlo studies of the adsorption of organic molecules in zeolites appear to predict preferred adsorption positions as well as heats of adsorption quite well, not withstanding the need for improvement of the potentials employed. The agreement of computed rates of diffusion of small organic molecules using Molecular Dynamic approaches with spectroscopic data can also be considered a significant accomplishment.

REFERENCES

1 D. Avnir, D. Farin and P. Pfeifer, J. Chem. Phys. 79(7), 3566 (1983).
2 W.M. Meier, Stud. Surf. Sci Catal. 28, (1986) 13.
3a Computer Simulation of Solids, (C.R.A. Catlow and W.C. Mackrodt, Eds) Lecture Notes in Physics 166, Springer-Verlag 1982;
b C.R.A. Catlow, M. Doherty, G.D. Price, M.J. Sanders and S.C. Parker, Materials Science Forum, 7, (1986) 163;
c R.A. Jackson and C.R.A. Catlow, Molecular Simulation 1, (1988) 207.
4a R.A. van Santen, A. de Man and B.W. van Beest, Proc. NATO ASI "Physicochemical properties of zeolitic systems and their low dimensionality", Dourdan, France, 1989;
b B.W. van Beest, J. van Lenthe and R.A. van Santen, in preparation.
5a K.T. No, H. Chon, T. Lee and M.S. Jhon, J. Phys. Chem. 85, (1981) 2065;
b K.T. No, J.S. Kim, Y.Y. Huh and M.S. Jhon, J. Phys. Chem. 91, (1987) 740.
6a J.E. Hurley, J. Phys. Chem. 69, (1985) 3284;
b R.T. Sanderson, Chemical Periodicity, Reinhold, New York, 1960;
c W.J. Mortier, Stud. Surf. Sci. Catal. 37, (1988) 253.
7 M.K. Song, H. Chon, M.S. Jhon and K.T. No, J. Mol. Catal. 47, (1988) 73.

8 C.J.J. den Ouden, R.A. Jackson, C.R.A. Catlow and M.F.M. Post, to be published.
9 G. Ooms, R.A. van Santen, C.J. J. den Ouden, R.A. Jackson and C.R.A. Catlow, J. Phys. Chem. 92, (1988) 4462.
10 N.L. Allinger, J. Am. Chem. Soc. 99, (1977) 8127.
11 M. Mabilia, R.A. Pearlstein and A.J. Hopfinger, J. Am. Chem. Soc. 109, (1987) 7960.
12 R.A. van Santen, G. Ooms, C.J.J. den Ouden, B.W. van Beest and M.F.M. Post, Proc. Symposium on Advances in Zeolite Synthesis ACS Meeting, Los Angeles, 1988.
13 A.J.M. de Man, B.H.W. van Beest, M. Leslie and R.A. van Santen, J. Phys. Chem. accepted.
14 K.J. Choi, M.S. Jhon and K.T. No, Bull. Korean Chem. Soc. 8, (1987) 155.
15 K.T. No, D.H. Bal and M.S. Jhon, J. Phys. Chem. 90, (1986) 1772.
16 C. Lee, J. Phys. Chem.: Solid State Phys. 19, (1986) 5555.
17 S.H. Garofalini, J. Non-Crystalline Solids 55, (1983) 451.
18 E. Clementi, Computational Aspects of Large Chemical Systems, Springer-Verlag, Berlin, 1980.
19 B.M. Axilrod and E. Teller, J. Chem. Phys. 11, (1943) 299.
20 S.H. Garofalini, J. Am. Cer. Soc. 67, (1984) 133.
21a T.F. Soules, J. Chem. Phys. 71, (1979) 4570;
b S.H. Garolini, J. Chem. Phys. 76, (1982) 3189.
22 C. Pisani, R. Dovesi and C. Roetti, Hartree-Fock ab-initio treatment of crystalline systems, Lecture Notes in Chemistry 48, Springer-Verlag, 1988.
23 M.D. Newton. M. O'Keeffe and G.V. Gibbs, Phys. Chem. Minerals 6, (1980) 305.
24 S. Tsuneyuki, M. Tsukada, H. Aoki and Y. Matsui, Phys. Rev. Lett. 61, (1988) 869.
25 B. van Beest and R.A. van Santen, Catal Lett. 1, (1988) 147.
26 A.G. Pelmenschikov, E.A. Paukstitis, V.S. Stepanov, K.G. Ione, G.M. Zhidoniroy and K.I. Zamaraev, Proc. 9th Int. Congr. Catal. 1, (1988) 404, The Chemical Institute of Canada
27 E.G. Derouane and J.G. Fripiat, Zeolites 5, (1985) 165.
28 P.J. O'Malley and J. Dwyer, Zeolites 8, (1988) 317.
29 S. Beran, J. Phys. Chem. 137, (1983) 89.
30 J. Sauer, H. Haberlandt, W. Schirmer and P.A. Jacobs et al. (Eds.) Proc. of the Conference on Structure and Reactivity of Modified Zeolites, Prague, 1984, Elsevier, Amsterdam, 1984.
31a P. Hotza, J. Sauer, C. Morgeneyer, J. Huych and R. Zahradnik, J. Phys. Chem. 85, (1981) 4061;
b J. Sauer, C. Morgeneyer and R.P. Schroder, J. Phys. Chem. 88, (1984) 6375;
c J. Sauer and R. Zahradnik, Int. J. Quantumchem. 26, (1984) 739;
d J. Sauer, Acta Phys. Chem. 31, (1985) 19;
e J. Sauer and K.P. Schroder, Z. Phys. Chem. Leipzig 266, (1985) 379;
f J. Sauer, J. Phys. Chem. 91, (1987) 2315.
32 P. Hobza and R. Zahradnik, Chem. Rev. 88, (1988) 871.
33 H. Tatewaki and S. Huzinaga, J. Chem. Phys. 71, (1979) 4339.
34 S.F. Boys and F. Bernardi, Mol. Phys. 19, (1970) 553.
35a K.L. Miller, Biopolymers 18, (1979) 959;
b J.A. Yoffe, Theor. Chim. Acta 55, (1980) 219;
c Y.K. Kang and M.S. Jhon, Theor. Chim. Acta 61, (1982) 41.
36 G. Alagona and A. Tani, J. Chem Phys. 74, (1981) 3980.
37 C.E. Dykstra, Acc. Chem. Res. 21, (1988) 355
38 J. Snir, R.A. Nemenoff and H.A. Scheraga, J. Phys. Chem. 82, (1978) 2497.
39a A.G. Bezus, A.V. Kiselev, A.A. Lopatkin and P.Q. Du, J. Chem. Soc. Faraday Trans. II 74, (1978) 367;
b A.V. Kiselev and P.A. Du, J. Chem. Soc. Far. Trans. II 77, (1981) 1;
c A.V. Kiselev and P.A. Du, J. Chem. Soc. Far. Trans. II 77, (1981) 17;
d A.V. Kiselev, A.A. Lopatkin and A.A. Schulga, Zeolites, 5, (1985) 261.
40a J.G. Kirkwood, Phys. Z. 33, (1932) 57;
b A. Muller, Proc. Roy. Soc. A. 154, (1936) 624.

41a P.A. Wright, J.M. Thomas, A.K. Cheetham and A.K. Nowak, Nature 318, (1985) 611;
b A.K. Cheetham, A.K. Nowak and P.W. Betteridge, Proc. Ind. Acad. Sci. (Chem. Sci.) 96, (1986) 411.
42 S. Yashonath, J.M. Thomas, A.K. Nowak and A.K. Cheetham, Nature 331, (1988) 601.
43 B. Smit and C.J.J. den Ouden, J. Phys. Chem. 92, (1988) 7169.
44 L. Leherte, D.P. Vercauteren, E.G. Derouane and J.M. Andre, Stud. Surf. Sci. Catal. 37, (1988) 293.
45a A. Guirsot, F. Fajula, C. Daul and J. Weber, J. Phys. Chem. 92, (1988) 4456;
b J. Weber, P. Fluelinger, P.Y. Morgantini, O. Schaad, A. Guirsot and C. Daul, J. Computer Aided Molecular Design 92, (1988) 235.
46a G.M. Zhidomirov and V.B. Kazansky, Adv. Catal. 34, (1986) 131;
b P.A. Jacobs and W.J. Mortier, Zeolites 2, (1982) 226;
c J. Dwyer, Stud. Surf. Sci. Catal. 37, (1988) 333.
47 W.J. Mortier, J. Sauer, J.A. Lerchev and H. Noller, J. Phys. Chem. 88, (1984) 905.
48a P.J. O'Malley and J. Dwyer, J. Chem. Soc. Chem. Comm. 72 (1987);
48b P.J. O'Malley and J. Dwyer, J. Phys. Chem. 92, (1988) 3005.
49a E. Kassab, K. Seiti and M. Allavena, J. Phys. Chem. 59, *to appear*;
b K. Seiti, Thesis, Univ. Paris VI (1988).
50 R. Vetrivel, C.R.A. Catlow and E.A. Colbourn, Stud. Surf. Sci. Catal. 37, (1988) 37.
51 S. Beran, J. Phys. Chem. 89, (1985) 5586.
52 K. Mueller, H.J. Ammann, D.M. Doran, P. Gerber and G. Schrepfer, Innovative Approaches in Drug Research, A.F. Harms (Ed.), Elsevier, Amsterdam, 1986.
53 T. Gund and P. Gund, Molecular Structure and Energetics Vol. 4, J.F. Liebman and A. Greenberg (Eds.), VCH Publishers, New York, 1987.
54 U. Bunkert and N.L. Allinger, Molecular Mechanics, ACS Monograph No. 177, Washington DC, 1982.
55 H.J.C. Berendsen, J. Computer Aided Molecular Design 2(3), (1988) 217.
56 C. Hansch, Molecular Structure and Energetics, Vol. 4, J.F. Liebman and A. Greenberg (Eds.), VCH Publishers, New York, 1987.
57 T. Clark, A Handbook of Computational Chemistry, Wiley, New York, 1985.
58 S. Ramdas, J.M. Thomas, P.W. Betteridge, A.K. Cheetham and E.K. Davies Angew. Chem. Int. Ed. Engl. 23, (1984) 671.
59 E. Keller, J. Appl. Cryst. 22, (1989) 19.
60 M.J. Connoly, Science 221, (1983) 709.
61 Visualization in Scientific Computing, B.C. McCormick, T.A. DeFanti and M.D. Brown (Eds.), Computer Graphics, Vol. 21, (1987).
62 R.A.J. Driessen, B.O. Loopstra, D.P. de Bruijn, H.P.C.E. Kuipers and H. Schenk, J. Computer Aided Molecular Design, 2(3), (1988) 225.
63 S. Ramdas, J. Computer Aided Molecular Design, 2(4), (1988) 137.
64 J.V. Smith and W.J. Dytrych, Nature 309, (1984) 607.
65 D.E. Akporiaye and J.M. Thomas, submitted for publication.
66a S. Andersson, S.T. Hyde and H.G. von Schnering, Z. Kristallogr. 168, (1984) 1;
b H.G. von Schnering and R. Nesper, Angew. Chem. 99, (1987) 1097.
67 P.A. Wright, J.M. Thomas, A.K. Cheetham and A.K. Nowak, Nature 318, (1985) 611.
68 G.R. Millward, S. Ramdas, J.M. Thomas and M.T. Barlow, J. Chem. Soc. Faraday Trans. 79, (1983) 1075.
69 J.L. Schlenker, Zeolites 5 (1985), 346, 349, 352, 355.
70 M.M.J. Treacy and J.M. Newsam, Nature 332, (1988) 249.
71 M. Fujinaga, P. Gros and W.F. van Gunsteren, J. Appl. Cryst. 22, (1989) 1.
72 J.J. Keijsper, C.J.J. den Ouden and M. Post, 8th Int. Zeolite Conf., Amsterdam (1989).
73 I.E. Maxwell, J. Incl. Phenom. 4(1), (1986) 1.
74 E.F. Vansant, Proc. Int. Symp. on Innovation in Zeolite Materials Science, Elsevier, Amsterdam, 1988, p 143.

75 C. Mirodatos and D. Barthomeuf, J. Catalysis, 93, (1985) 246.
76 N. Metropolis, A.W. Rosenbluth, M.N. Rosenbluth, A.H. Teller and E. Teller, J. Chem. Phys. 21, (1953) 1081.
77 K. Binder, Introduction: Theory and Technical Aspects of Monte Carlo Simulations, in: Monte Carlo Methods, Springer-Verlag, Berlin, 1981.
78 N.G. van Kampen, Stochastic Processes in Physics and Chemistry North Holland, Amsterdam, 1980.
79 M.P. Allen and D.J. Tildesley, Computer Simulation of Liquids, Clarendon Press, Oxford, 1987.
80 J. Crank, The Mathematics of Diffusion, Clarendon Press, Oxford, 1975
81 O. Matsuoka, E. Clementi and M. Yoshimine, J. Chem. Phys. 77, (1982) 899.
82 L. Leherte, G.C. Lie, K.N. Swamy, E. Clementi, E.G. Derouane and J.M. Andre, Chem. Phys. Lett. 145(3), (1988) 237.
83 S. Yashonath, P. Demontis and M.L. Klein, Chem. Phys. Lett. 153(6), (1988) 551.
84 C.J.J. den Ouden, B. Smit, A.F.H. Wielers, R.A. Jackson and A.K. Nowak, Molecular Simulation, in press (1989)
85 R.L. June, A.T. Bell and D.N. Theodorou, 196th ACS National Meeting, Los Angeles, California, (September 1988).
86 M.G. Palekar and R.A. Rajadhyaksha, Chem. Eng. Sci. 40(7), (1985) 1085.
87 K.K. Pitale and R.A. Rajadhyaksha, Curr. Sci. 57(4), (1988) 172.
88 E.G. Derouane, J.M. Andre and A.A. Lucas, Chem. Phys. Lett. 137(4), (1987) 336.
89 E.G. Derouane, J.B. Nagy, C. Fernandez, Z. Gabelica, E. Laurent and P. Maljean, Appl. Catal. 40(1-2), (1988) 1.
90 E.G. Derouane, J.M. Andre and A.A. Lucas, J. Catal. 110(1), (1988) 58.